Crosstalk between bone marrow-derived myofibroblasts and gastric cancer cells regulates cancer stemness and promotes tumorigenesis

Liming Zhu[#2], **Xiaojiao Cheng**[#1], **Jindong Shi**[2], **Lin Jiacheng**[1], **Gang Chen**[1,2], **Huanyu Jin**[2], **Anna B. Liu**[2], **Hyunseung Pyo**[2], **Jing Ye**[3], **Yanbo Zhu**[6], **Hong Wang**[2], **Haoyan Chen**[5], **Jingyuan Fang**[5], **Li Cai**[7], **Timothy C. Wang**[4], **Chung S. Yang**[2], and **Shui Ping Tu**[1,2]

[1]Department of Oncology, Renji Hospital, School of Medicine, Shanghai Jiaotong University, 200127, China

[2]Department of Chemical Biology, Ernest Mario School of Pharmacy, Rutgers, the State University of New Jersey, Piscataway, NJ 08854, USA

[3]Emergency Medicine, Ruijin Hospital, School of Medicine, Shanghai Jiaotong University, 200025, China

[4]Department of Medicine, College of Physicians & Surgeons, Columbia University, New York, NY 10032, USA

[5]Department of Gastroenterology, Renji Hospital, School of Medicine, Shanghai Jiaotong University, 200232, China

[6]Department of Pathology, Ruijin Hospital, School of Medicine, Shanghai Jiaotong University, 200025, China

[7]Department of Biomedical Engineering, Rutgers, The State University of New Jersey, Piscataway, NJ 08854, USA

[#] These authors contributed equally to this work.

Abstract

Corresponding Authors: Dr. Shui Ping Tu, Department of Oncology, Renji Hospital, School of Medicine, Shanghai Jiaotong University, 200127, China, tushuiping@yahoo.com. Telephone: (8621)68385623, **Dr. Chung S. Yang,** Department of Chemical Biology, Ernest Mario School of Pharmacy, Rutgers University, Piscataway, NJ 08854, USA, csyang@pharmacy.rutgers.edu, Telephone: (848) 445 5360, Fax: (732) 445 0687.

Bone marrow-derived cells play important roles in cancer development and progression. Our previous studies demonstrated that murine bone marrow-derived myofibroblasts (BMFs) enhanced tumor growth. In this study, we investigated the mechanisms of BMF actions. We found that co-injection of BMFs with gastric cancer cells markedly promoted tumorigenesis. Co-cultured BMFs or BMF-conditioned medium (BMF-CM) induced the formation of spheres, which expressed stem cell signatures and exhibited features of self-renewal, epithelial-to-mesenchymal transition and tumor initiation. Furthermore, CD44^{+} fractions in spheres were able to initiate tumorigenesis and reestablish tumors in serially passaged xenografts. In co-culture systems, BMFs secreted high levels of murine interleukin-6 (IL-6) and hepatocyte growth factor (HGF), while cancer cells produced high level of transformation growth factor-β1 (TGF-β1). BMF-CM and IL-6 activated BMFs to produce mHGF, which activated signal transducer and activator of transcription 3 (STAT3) and upregulated TGF-β1 in human cancer cells. In return, cancer cell-CM stimulated BMFs to produce IL-6, which was inhibited by anti-TGF-β1 neutralizing antibody. Blockade of HGF/Met, JAK2/STAT3 and TGF-β1 signaling by specific inhibitors inhibited BMF-induced sphere formation. STAT3 knockdown in cancer cells also inhibited BMF-induced sphere formation and tumorigenesis. Moreover, TGF-β1 overexpression in cancer cells was co-related with IL-6 and HGF overexpression in stromal cells in human gastric cancer tissues. Our results demonstrate that BMF-derived IL-6/HGF and cancer cell-derived TGF-β1 mediate the interactions between BMFs and gastric cancer cells, which regulate cancer stemness and promote tumorigenesis. Targeting inhibition of the interactions between BMFs and cancer cells may be a new strategy for cancer therapy.

Introduction

Accumulating evidence has shown that tumor stroma plays important roles in cancer initiation and progression [24]. Tumor stromal cells include bone marrow (BM)-derived myeloid cells and lymphoid cells, mesenchymal stem cells (MSCs), myofibroblasts and endothelial progenitor cells. However, the contributions of these different stromal cells to tumorigenesis remain unknown. The bone marrow-derived myofibroblasts (BMFs) , a major cell type of stromal cells [3], have been shown to constitute a MSC niche [25]. BMF infiltration to the gastric tissues is associated with gastric cancer development [29]. BMFs have also been demonstrated to enhance tumor development and invasion[17, 25]. However, the underlying mechanisms by which BMFs promote tumorigenesis remain largely unknown.

Cancer stem cells (CSCs) or CSC-like cells (CSC-LCs) have been shown to play important roles in tumorigenesis and tumor progression in many types of tumors [23, 32], including gastric cancer.[27] CSCs are a subpopulation of tumor cells and are featured by their capabilities of self-renewal and tumor initiation.[23] CSCs can be regulated by their stromal microenvironment [6,31]. Studies have shown that tumor stromal cells, including myofibroblasts [31], MSC [28] , endothelial cells [10] and tumor-associated macrophages [14] ,

induce CSC-like sphere formation of cancer cells. However, whether BMFs promote tumorigenesis by induction of CSC-LCs remains unclear.

The interactions between stromal cells and cancer cells play pivotal roles in tumorigenesis and metastasis.[6, 21]. Tumor myofibroblast-derived factors induced epithelial cell transformation in co-culture systems and tumorigenesis in xenograft models [13]. Conditional inactivation of the bone morphogenetic protein type II receptor in the stroma increased the myofibroblast population, causing colon epithelial hyperplasia.[2] Further studies have shown that MSC-derived IL-6 activates JAK2/STAT3 signaling in colon cancer cells and induces sphere formation of cancer cells [28]. Colon myofibroblast-secreted HGF was shown to reprogram differentiated colon cancer cells to CSC-LCs through AKT/Wnt signaling [31]. Our previous studies showed that BMFs secreted higher levels of cytokines (e.g. IL-6), chemokines (e.g. SDF1), growth factors (e.g. IGF2), and matrix metalloproteinases (MMPs) (e.g. MMP13), and exhibited stronger capabilities of tumorigenesis and tumor invasion than resident fibroblasts [25]. Nevertheless, out of these factors derived from BMFs, the factors that mediate the activation of cancer cells remain to be investigated. In return, how cancer cells regulate BMFs is also largely unknown.

In this study, we investigated the interactions between BMFs and gastric cancer cells. Our results showed that BMF-derived IL-6 and HGF and cancer cell-derived TGF-β1 mediated the interactions between BMFs and cancer cells, and these interactions contribute to the induction of CSC-LCs and promote tumorigenesis.

Results

BMFs promote tumorigenesis of gastric cancer cells

Our previous study has shown that BMFs have stronger capacity to enhance tumor growth than wild type fibroblasts [25]. We then further focused on the study of the effects of BMFs on tumorigenesis in mice injected with small number of cancer cells. We found that BMFs enhanced tumorigenesis and tumor growth when BMFs were co-injected with 10^4 gastric cancer cell MFC into mice (Fig. 1A). Immunofluorescence (IF) staining showed a number of $EGFP^+\alpha\text{-}SMA^+$ cells (yellow cells) in tumor tissues from mice co-injected with mouse gastric cancer MFC cells and BMFs ($EGFP^+$), but not in tumor tissues from mice injected with MFC cells alone (Fig. 1B and supplementary Fig. 1A), suggesting that BMFs can retain in the tumors and promote tumor growth. Quantification analysis showed that the number of $\alpha\text{-}SMA^+$ (included $EGFP^+\alpha\text{-}SMA^+$ and $EGFP^-\alpha SMA^+$) was significantly higher in tumor tissues from mice co-injected with MFC cells and BMFs than in tumor tissues from mice injected with MFC cells alone (Supplementary Fig. 1A), suggesting that BMFs facilitate to recruit more myofibroblasts and promote tumor growth. The capability of BMFs to enhance tumorigenesis was further assessed with the highly tumorigenic MKN45 and weakly tumorigenic MKN28 cells. MKN45 cells and MKN28 cells at the number of 10^4 were injected alone or together with BMFs into NOD/SCID mice. We found that 40% of mice injected with 10^4 MKN45 cells developed tumors, while 80% of mice co-injected with 10^4 MKN45 cells and 10^4 BMFs developed tumors (Fig. 1C). While only 10% of mice injected with 10^4 MKN28 cells formed tumors, 60% mice co-injected with 10^4 MKN28 cells and BMFs developed tumors (Fig. 1D). Our previous study showed that $CD44^+$ gastric cancer

cells were stem cells (CSCs), whereas CD44^{−} MKN45 cells were non-CSCs and could not form spheres[27]. We found that BMFs also enhanced tumorigenesis in CD44^{−} MKN45 cells (Fig. 1E). However, mice injected with BMFs (2×10^6 cells) alone did not form tumors (data not shown). The results demonstrate that the co-injected BMFs *in vivo* promote tumorigenesis.

BMFs induce sphere formation of gastric cancer cells

To investigate whether BMF-promoted tumorigenesis is due to inducing CSCs, we determined the effects of BMFs on stem-like sphere formation. When co-cultured with BMFs, MKN45 cells (95% of which were CD44^{+} cells) formed more and larger spheres than MNK45 cells cultured alone (Fig. 1F). The co-cultured BMFs also induced sphere formation of mouse gastric cancer MFC cells (Fig. 1G), human colon cancer cells SW620, and liver cancer HepG2 cells (Supplementary Fig. 1B). We further explored whether BMFs induce non-CSCs to form spheres. We sorted CD44^{+} and CD44^{−} MKN45 cells and co-cultured them with BMFs. Both CD44^{+} and CD44^{−} MKN45 cells formed more spheres when co-cultured with BMFs, compared to those cultured alone (Supplementary Fig. 1C). Flow cytometry (FACS) analysis showed that 11.5% of CD44^{−} MKN45 cells became CD44^{+} cells after co-culturing with BMFs, but very few CD44^{−} cells became CD44^{+} cells when cultured alone (Supplementary Fig. 1D-1E). To further investigate the effects of BMFs on non-CSCs, by using CD44 deficient (CD44^{−}) MKN28 gastric cancer cells[27]. We observed that MKN28 cells (EGFP^{−} cells) formed spheres when co-cultured with BMFs (EGFP^{+} cells), while MKN28 cells cultured alone in Stem Cell Medium (SCM) did not (Fig. 1H). The results indicate that BMFs induce sphere formation of CD44^{−} non-CSCs.

To determine whether BMF-induced sphere formation is independent on cell-cell contact, we used a transwell co-culture system in which MKN28 cells and BMFs were seeded separately into lower and upper transwells (Supplementary Fig. 2A). The 0.4 μm filter between the two wells blocks cell penetration but allows media communication. The indirectly co-cultured MKN28 cells with BMFs formed more and larger spheres than MKN28 cells indirectly co-cultured with the control HEK293 cells (Supplementary Fig. 2A). Furthermore, BMF-CM and Co-culture-CM significantly increased the sphere formation of MFC, MKN28 and MKN45 cells compared to the SCM, and Co-culture-CM exhibited the strongest induction of sphere formation (Fig. 1G and Supplementary Fig. 2B-2C). The results suggest that BMF-derived factors contribute to the sphere formation of cancer cells.

BMF-induced spheres exhibit CSC properties

To determine whether BMF-induced spheres have CSC properties, we digested spheres into single cells and seeded the single cells into ultralow attachment plates. We observed that BMF-CM-induced MKN28 spheroid cells (first generation spheres) formed second generation spheres in SCM (Fig. 2A-2B), confirming that BMF-induced MKN28 spheres (referred to as MKN28-CSC-LCs) possess the self-renewal feature, one of the CSC properties. When cultured in attachment culture plates, the MKN28-CSC-LCs exhibited mesenchymal-like morphology, while the parental MKN28 cells did not (Fig. 2A). When cultured in SCM, MKN-28-CSC-LCs form more spheres than MKN-28 cells (Fig. 2B).

Western blot showed that the expression of vimentin, snail and TGF-β1 was higher, while the expression of E-cadherin was lower in MKN28-CSC-LCs than those in parental cells (Fig. 2C). These results indicate that MKN28-CSC-LCs possess EMT characteristics, one of CSC features [22]. Microarray analysis showed that BMF-induced MKN28-CSC-LCs overexpressed multiple signaling molecules of CSCs (Supplementary Fig. 3A), including CD10 (breast tissues stem cell and breast cancer stem cell marker) [20], KIAA1199 (Wnt/β-catenin pathway) [4], Hey-1 (Notch signaling) and DUSP6 (STAT3 signaling). RT-PCR confirmed that the expression of CD10, KIAA119, Hey-1 and DUSP6 was significantly increased in MKN28-CSC-LCs compared to those in parental MKN28 cells (Supplementary Fig. 3B).

To investigate the *in vivo* tumorigenic capability of BMF-induced CSC-LCs, different numbers of MKN28-CSC-LCs were injected into NOD/SCID mice. Mice injected with 10^2, 10^3, 10^4 and 10^5 MKN28-CSC-LCs developed tumors 3 months after the injection, while none of the mice injected with 1×10^5 MKN28 parental cells formed tumor (Fig. 2D). To test whether parental MKN28 cells are tumorigenic, we injected different numbers of MKN28 cells into mice and found that mice injected with 2×10^5 and 1×10^6 MKN28 cells could form tumors 3 months after the injection (Supplementary Fig. 2D). These data demonstrate that parental MKN28 cells are tumorigenic and that MKN28-CSC-LCs initiate tumorigenesis.

To investigate whether BMF-induced CD44$^+$ cells in spheres contribute to tumorigenesis, we sorted CD44$^+$ and CD44$^-$ cells from the spheres formed from CD44$^-$ MKN45 cells co-cultured with BMFs. Different numbers of CD44$^+$ and CD44$^-$ spheroid cells were injected into NOD/SCID mice. Mice injected with 10^2, 10^3 and 10^4 CD44$^+$ spheroid cells respectively, had tumor incidences of 20%, 60% and 80%, whereas mice injected with 10^4 CD44$^-$ spheroid cells did not form tumors (Fig. 2E). The result suggests that CD44$^+$ cells in spheres initiate tumorigenesis. To further confirm that CD44$^+$ cells possess self-renewal function *in vivo*, we performed serial transplantation by injecting the re-isolating CD44$^+$ cells from first transplants (tumors) into recipient SCID mice (as second transplants). The mice injected with 10^3 and 10^4 CD44$^+$ xenograft tumor cells had tumor incidence of 40% and 60%, whereas mice injected with 10^4 CD44$^-$ tumor cells did not formed tumor (Fig. 2F). These xenograft tumors of both first and second transplants showed the same histology and expressed CD44$^+$ in *vivo* (Fig. 2G). These results demonstrate that CD44$^+$ cells are able to re-establish tumor, to self-renew and sustain tumor growth in serially passaged xenografts. Taken together, these results indicate that BMF-induced CD44$^+$ fraction in spheres are gastric cancer stem cells.

BMF-derived IL-6 induces sphere formation of mouse cancer cells

The above results suggest that BMF-derived factors contribute to the induction of CSC-LCs. To identify these factors, we conducted antibody array analysis of BMF-CM and Co-culture-CM of BMFs and MKN28 cells. The result showed that murine (m) IL-6 level was significantly higher in Co-culture-CM than that in BMF-CM (Fig. 3A). ELISA assay confirmed the results of the array (Fig. 3B). RT-PCR also demonstrated that BMFs, co-cultured with MKN28 cells, expressed higher level of IL-6 mRNA than BMFs alone did

(Supplementary **Fig. 4A**). Similar elevation of IL-6 level was obtained in the BMFs co-cultured with human AGS cells (Supplementary **Fig. 4B**). However, the levels of mIL-β1 and mTNF-α were low and not affected by co-culturing (Fig. 3A). In addition, we determined the level of human IL-6 (hIL-6) in culture medium and found that the level of hIL-6 did not significantly increased in co-culture medium compared to cancer cell medium (Supplementary Fig. 4C), suggesting that mouse IL-6, but not human IL-6 plays a major role in mediating the interactions between BMFs and cancer cells. Using this co-culture system of murine BMFs and human cancer cells, the cell origins of cytokines, chemokines and growth factors were readily distinguished using human or mouse specific antibodies or primers for PCR. Similarly, the co-culturing of BMFs with mouse MFC cells significantly increased mIL-6 level (Fig. 3C). These results demonstrate that cancer cells activate BMFs to produce mIL-6 in the co-culture system.

We then studied the role of BMF-derived IL-6 in sphere formation of cancer cells. The pre-incubation of BMF-CM or Co-culture-CM with mIL-6 neutralizing antibody significantly decreased sphere formation of mouse MFC cells (Fig. 3D), but did not affect sphere formation of human MKN28 cells (Supplementary Fig. 4D). These results suggest that mIL-6 did not involve in mBMF-induced sphere formation of human cancer cells. However, JSI-124 (a JAK2 inhibitor) significantly reduced BMF-induced sphere formation in both MKN28 cells and MFC cells (Fig. 3E), suggesting the involvement of JAK2/STAT3 pathway in the sphere formation of human cancer cells. Although TIMP-2 was also significantly increased in Co-culture-CM (Fig. 3A), anti-TIMP-2 antibody did not block BMF-CM or Co-culture-CM-induced sphere formation of MFC cells(data not shown), indicating that TIMP-2 is not involved in induction of CSCs.

BMF-derived HGF induces sphere formation of human cancer cells

To determine which BMF-derived factors contribute to the sphere formation of human cancer cells, we first examined expressions of cytokines, including SCF, IL-11 and IL-10, which are known to activate STAT3[8]. RT PCR showed that the mHGF mRNA expression was significantly higher in BMFs co-cultured with human MKN28 cells than that in BMFs cultured alone (Supplementary Fig. 4A), whereas the expressions of SCF, IL-11 and IL-10 were not different in the co-cultured BMFs compared to the BMFs cultured alone (data not shown). ELISA assay showed that the mHGF level was significantly higher in the Co-culture-CM of MKN-28 cells and BMFs than that in BMF-CM of BMFs alone (Fig. 4A). Elevated mHGF was also observed in Co-culture-CM of BMFs and mouse MFC cells (Supplementary Fig. 5A), suggesting that mHGF was generally involved. To determine the effect of HGF/Met signaling on sphere formation, we used crizotinib, a Met kinase inhibitor[19], to block HGF/Met signaling. Crizotinib treatment significantly reduced BMF-induced sphere formation in MKN28 and MKN45 cells (Fig. 4B), suggesting that murine BMF-derived HGF is a key factor inducing sphere formation of human cancer cells.

We noted that the elevated expression of mHGF was parallel with the increased expression of mIL-6 in BMFs (Supplementary Fig. 4A) and hypothesized that IL-6 induced HGF expression in BMFs. We found that both recombinant mIL-6 (rmIL-6) and rhIL-6 treatment significantly increased the mRNA expression of mHGF (Fig. 4C) and protein levels of p-

JAK2 and p-STAT3 in BMFs (Fig. 4D). BMF-CM and rmIL-6 treatment stimulated BMFs to secrete mHGF, while these actions were inhibited by JSI-124 (Fig. 4E). These results suggest that BMF-derived IL-6 stimulates BMFs to produce mHGF through the JAK2/ STAT3 pathway.

We then investigated the roles of IL-6 and HGF in sphere formation. We found that rhIL-6 or rhHGF treatment induced sphere formation of MKN28 cells and that the combination of rhIL-6 and rhHGF exhibited stronger induction of sphere formation than rhIL-6 or rhHGF alone did (Fig. 4F). Similar results were obtained in MFC cells when treated with rIL-6 and rHGF (Supplementary Fig. 5B). Moreover, rmIL-6 and rmHGF treatment upregulated CD44 expression in MFC cells (Fig. 4G) and increased the percentage of CD44$^+$ cells (Fig. 4H), consistent with the results shown above (Supplementary Fig.1C-1D). Furthermore, the combination of JSI-124 and crizotinib significantly inhibited BMF-induced sphere formation of MFC cells than JSI-124 or crizotinib alone (Supplementary Fig. 5C). These results indicate that BMF-derived HGF directly induces sphere formation of human cancer cells, and that BMF-derived IL-6 indirectly contributes to sphere formation of human cancer cells *via* the upregulation of mHGF in BMFs.

The activation of STAT3 contributes to BMF-induced sphere formation and tumorigenesis

To investigate the mechanisms by which BMF-derived IL-6 and HGF induce sphere formation, we treated cancer cells with BMF-CM and found that BMF-CM treatment increased the levels of p-STAT3 and p-Met in MKN28 gastric cancer cells (Fig. 5A). Since mIL-6 is inactive to human cancer cells, we proposed that mHGF in BMF-CM may contribute to the STAT3 activation in human cancer cells. Consistent with this hypothesis, rmHGF treatment increased the levels of p-Met and p-STAT3 in human cancer MKN28 cells (Fig. 5B), whereas crizotinib inhibited BMF-CM-induced expressions of p-Met and p-STAT3 in human gastric cancer cells (Fig. 5C). These results suggest that BMF-derived HGF activates STAT3 and Met signaling in human gastric cancer cells.

To determine the role of STAT3 in BMF-induced sphere formation, we established stable STAT3-knockdown MKN28 colonies (Supplementary Fig. 6A). STAT3 knockdown in MKN28 cells significantly reduced rhIL-6-induced levels of p-STAT3 and TGF-β1 (Fig. 5D) and inhibited BMF-CM-induced sphere formation (Fig. 5E). Furthermore, STAT3 knockdown in MKN28 cells inhibited BMF-promoted tumorigenesis and tumor growth in xenograft models (Fig. 5F and Supplementary Fig. 6B). The results demonstrate that BMF-derived IL-6/HGF activate STAT3, which induces sphere formation and tumorigenesis.

Cancer cell-derived TGF-β1 activates BMFs

The above results that BMF-induced spheres expressed high level of TGF-β1 (Fig. 2C) and that co-cultured cancer cells stimulated BMFs to produce mIL-6 (Fig. 3A-3C) suggest tumor-derived TGF-β1 as a key factor that activates BMFs. Indeed, ELISA showed that hTGF-β1 level was significantly higher in Co-culture-CM than the level in MKN28-CM, MKN45-CM and MFC-CM (Fig. 6A-6C), whereas the levels of hIL-1β, hIL-6, and hTNF-α remained low (data not shown). Furthermore, the pre-incubation of anti-human TGF-β1 neutralizing antibody reduced MKN28-CM and Co-culture-CM-induced mIL-6 production

in BMFs (Fig. 6D). SB-505124 (a TGF-β type I receptor inhibitor) treatment also decreased MKN28 cell-induced mIL-6 production in BMFs (Fig. 6E). Treatment of gastric cancer cells with SB-505124 significantly reduced BMF-induced sphere formation (Fig. 6F). These results demonstrate that cancer cell-derived TGF-β1 activates BMFs in a co-culture system.

Overexpressions of hTGF-β1 and hIL-6 in human gastric cancer tissues

To extend our findings to human samples, we investigated the correlation among TGF-β1, IL-6 and HGF in 41 human gastric cancer tissues (Supplementary Table 1). IHC staining showed that overexpression of hTGF-β1 was observed mainly in cancer cells, while the expression of hIL-6 and hHGF was observed in both stromal cells and cancer cells (Fig. 7A). Fifteen out of 41 samples showed high expression of hTGF-β1 and 12 samples showed high expression of hIL-6. Also, 10 samples showed high expression of both hTGF-β1 and hIL-6, and 12 samples showed high expression of both hTGF-β1 and hHGF (Supplementary Table 2). Significant correlations between IL-6 and TGF-β1 expressions, as well as between HGF and TGF-β1 expression were found (Supplementary Table 2, P < 0.05). The normal gastric tissues showed only weak hTGF-β1 expression, and all normal samples showed no hIL-6 and hHGF expression (Fig. 7A). In addition, we analyzed data from 230 patients with gastric cancer deposited in the Cancer Genome Atlas (TCGA-BR-A4PE) database (Cancer Genome Atlas Network). The expression of HGF was positively correlated with IL-6 expression (Fig. 7B). The expression of TGF-β1 was positively correlated with the expression of IL-6 and HGF (Fig. 7C-7D). These results support our proposal that the IL-6/HGF and TGF-β signaling loop is also active in primary human gastric cancers and contributes to the interactions between BMFs and cancer cells, which promote tumor growth.

Discussion

In this study, we demonstrated that BMFs could induce non-CSCs to form CSC-LCs. BMF-derived IL-6 and HGF activated STAT3 in cancer cells, resulting in the upregulation of TGF-β1 in cancer cells. In return, cancer cell-derived TGF-β1 activated BMFs to produce higher levels of IL-6 and HGF. Furthermore, the inhibition of IL-6/STAT3 and HGF/c-Met signaling in BMFs and TGF-β1 signaling in cancer cells significantly inhibited BMF-induced reprogramming of non-CSCs to CSC-LCs and tumorigenesis. Our results reveal a new crosstalk between BMFs and cancer cells in promoting tumorigenesis through an IL-6/HGF and TGF-β1 signaling loop.

Tumor stroma has been shown to play an important role in the induction of CSCs.[16] Our results, for the first time, demonstrated that BMFs induced CSC-LCs in gastric cancer cells and that the BMF-induced CSC-LCs have CSC properties. The evidence includes: (1) BMF-induced CSC-LCs are similar to CSCs in the ability of self-renewal; (2) BMF-induced CSC-LCs possess the features of EMT linked to CSCs;[26] (3) BMFs or BMF-derived IL-6 and HGF increased expression of CD44^{+}, a stomach CSC marker; (4) CD44^{+} cells, but not CD44^{−} cells, isolated from spheres developed tumors; (5) BMF-induced CSC-LCs overexpress multiple signaling molecules of CSCs, including KIAA1199, CD10 and TGF-β1; (6) BMF-reprogrammed CSC-LCs exhibit tumor initiation and capabilities of CSCs in

serial tumor transplant experiment. Our results reveal a new mechanism for BMFs to induce CSCs to promote tumor genesis.

Serum IL-6 level has been shown to be associated with gastric cancer progression. Our observation that the IL-6 level was significantly increased in the BMFs co-cultured with cancer cells suggests that IL-6 is a major BMF-derived factor induced by cancer cells. The role of IL-6 in activating the JAK2/STAT3 pathway in mouse MFC cells is demonstrated by pre-treatment with anti-mouse IL-6 neutralizing antibody, which significantly inhibited the effect of BMF-CM on activation of JAK2/STAT3 signaling. STAT3 knockdown also significantly reduced BMF-CM-induced activation of JAK2/STAT3 in mouse MFC cells. These results demonstrate that STAT3 activation is a key event for BMF-induced CSC-LCs. We also noted that anti-mouse IL-6 neutralizing antibody did not affect the BMF-CM-induced sphere formation of human cancer cells, due to the fact that mIL-6 can not activate human IL-6 receptor.[11] Nevertheless, the BMFs induced the sphere formation of human cancer cells, and the addition of JAK2 inhibitor or the STAT3 knockdown significantly inhibited BMF-CM or BMF-induced sphere formation of human cancer cells. The results suggest that other factors derived from BMFs activate STAT3 in human cancer cells. Other than IL-6, STAT3 can be activated by other cytokines and growth factors including HGF, SCF, IL-11 and IL-10 [8]. Our findings that BMF-derived HGF induces sphere formation of human cancer cells is supported by the observation: (1) mHGF was significantly increased in Co-culture-CM; (2) rmHGF activated STAT3 signaling in human gastric cancer cells; (3) Met inhibitor significantly suppressed BMFs and BMF-CM-induced sphere formation and STAT3 activation in human cancer cells.

In this study, an important finding is that BMF-derived IL-6 activates BMFs to produce mHGF. We found that both rmIL-6 and rhIL-6 activated JAK2/STAT3 signaling and stimulated mHGF expression in BMFs and that the blockade of JAK2/STAT3 signaling reduced HGF production. HGF has been shown to activate JAK2/STAT3 signaling in liver cells [18]. Myofibroblasts-derived HGF has been shown to reprogram colon CSC-LCs through the activation of Wnt signaling.[31] Our results indicate that BMF-derived HGF can activate STAT3 in gastric cancer cells, and BMF-derived IL-6 indirectly contributes to the induction of CSC-LCs through upregulation of HGF. rIL-6 and rHGF could upregulate expression of CD44 in gastric cancer cells, consistent with a recent report (42). Our results, for the first time, showed that IL-6 and HGF cooperated to induce sphere formation of cancer cells, highlighting the important roles of IL-6 and HGF in tumorigenesis.

We also demonstrated that gastric cancer cells could, in return, activate BMFs. It has been reported that TNF-α and IL-1β activate myofibroblasts, resulting in the production of IL-6.[7, 9] TGF-β signaling has been shown to play important roles in the regulation of stemness,[33] EMT[34] and differentiation of fibroblasts.[15] Our finding that gastric cancer cell-derived TGF-β1 activated BMFs is supported by the results that (1) the level of hTGF-β1, but not the levels of hIL-1β and TNF-α, was significantly increased in Co-culture-CM; (2) cancer cell-CM and Co-culture-CM significantly induced mIL-6 production in BMFs, and anti-human TGF-β1 neutralizing antibody inhibited their effects; (3) TGF-β1 receptor inhibitor SB505124 reduced BMF-induced sphere formation of cancer cells; (4) BMF-induced CSC-LCs highly expressed TGF-β1; (5) co-overexpression of hTGF-β1 and hIL-6

was found in human gastric cancer tissues. Our results are similar to the recent reports that colon cancer-derived TGF-β activates myofibroblasts, resulting in enhanced tumor growth, invasion and metastasis[125] .

In summary, we demonstrate for the first time that BMF-derived IL-6 and HGF activate STAT3 in cancer cells to secrete TGF-β1, and BMF-derived IL-6 also activates BMFs to produce HGF. In return, cancer cell-derived TGF-β1 stimulates BMFs to produce IL-6 and HGF, constituting a positive signaling loop that mediates the interactions between BMFs and cancer cells and contributes to upregulating CD44 expression and regulating cancer stemness (Fig. 7E). Our results provide new insights into the mechanisms by which BMFs promote tumorigenesis and suggest potential molecular targets for the prevention and treatment of cancer by inhibiting the interactions between BMFs and cancer cells

Materials and Methods

Cell culture and reagents

Human gastric cancer MKN45 cells and MKN28 cells (RIKEN, Japan), AGS cells (ATCC, Manassas, VA), SGC-7901 cells and mouse gastric cancer MFC cells (Cell Bank, Shanghai), human colon cancer SW620 cells and human liver cancer cells HepG2 (ATCC, Manassas, VA), were maintained in RPMI-1640 media containing 10% FBS, 100 U/mL penicillin, and 100 μg/mL streptomycin (Gibco BRL). BMFs (EGFP$^+$) that were freshly isolated from gastric dysplastic tissues of IL-1β transgenic mice [29] transplanted with EGFP$^+$ bone marrow according to our previous method [25]. All cell lines were tested for *mycoplasma* by a PCR method (Stratagene), and all cell lines were *mycoplasma* negative. BMFs within 12 generations were used. JSI-124 and NSC33994 (JAK2 inhibitor), crizotinib (c-Met inhibitor) and SB-505124 (TGF-β1 type I receptor inhibitor) were purchased from Sigma and Tocris (R&D Systems), dissolved in dimethyl sulfoxide (DMSO) and stored at −20°C. Human (h) and mouse (m) recombinant (r) IL-6 and HGF purchased from Peprotech (Rocky Hill,NJ). The anti-mouse IL-6 neutralizing antibody (Cat. MAB406) and anti-human TGF-β1 antibody (Cat. MAB7364) neutralizing antibodies were purchased from R&D Systems (Minneapolis, MN, Indiana).

Sphere Formation Assay

Stem cell medium (SCM) was prepared by adding basic fibroblast growth factor (bFGF; 10 ng/mL) and epidermal growth factor (EGF; 20 ng/mL) (PeproTech, Rocky Hill, NJ) to the RPMI 1640 medium (Gibco, Grand Island, NY) containing 0.1% bovine serum album (BSA). To prepare BMF-conditioned medium (BMFCM), 1.5×10^6 BMFs were cultured in 10 mL of serum-free RPMI medium without EGF and bFGF for 24 hours. BMF-CM was collected and stored at −20°C. To prepare co-culture medium of BMFs and cancer cells (Co-culture-CM), 1×10^6 BMFs and 1×10^6 cancer cells were co-cultured in 10 mL of serum-free RPMI 1640 medium without EGF and bFGF for 24 hours. The Co-culture-CM was collected and stored at −20°C.

Cancer cells (1×10^4) were cultured alone or co-cultured with BMFs (2×10^4) in SCM in a 6-well plate for 2 weeks. For an indirect co-culture system, cancer cells and BMFs were

separately seeded in lower wells and upper transwells (diameter 0.4 μM, Corning) in SCM for 2 weeks. In other experiments, cancer cells (1×10^2) were seeded in an ultralow attachment 96-well plate and cultured with SCM or BMF-CM for 2 weeks. Each group included triple wells and experiments were repreated three times (n=9). Spheres were recognized as a 3-dimensional spherical structure composed of cell colonies. The number of spheres in the entire well was counted, and the percentage of total sphere numbers to the total seeded cells is referred to as "sphere ratio".

Antibody array

BMFs (1×105) and MKN28 cells (1×105) were cultured alone or together in 2 ml of RMPI 1640 complete medium in a 6-well plate. Twenty-four hours later, cells were washed twice with PBS and incubated with fresh serum-free RMPI 1640 for another 24 hours. Then, the BMF-conditioned medium (BMF-CM), MKN28-CM and Co-Culture-CM were collected for antibody array. The mouse cytokine/chemokine array kits (Ray Biotech Inc. Atlanta, GA) were used to detect a panel of 24 secreted cytokines and chemokines in BMF-CM and Co-Culture-CM. The human cytokine/chemokine array kits (Ray Biotech Inc.) were used to detect a panel of 24 secreted cytokines and chemokines in MKN28-CM and Co-Culture-CM according to the manufacturer's recommended protocol. The spot signal densities of array membrane were scanned using the Odyssey Infrared Imaging System (Li-Cor Biosciences). The raw numerical densitometry data were extracted from background. The data of samples were normalized to the positive control signals. The signal intensity for each antigen-specific antibody spot was proportional to the relative concentration of the antigen in that sample. The experiments were repreated twice (n=3).

Enzyme-linked immunosorbent assay (ELISA)

BMFs (1×10^5) and cancer cells (1×10^5) were cultured alone or together in 2 ml of RPMI-1640 complete medium in a 6-well plate for 48 hours. The BMF-CM, cancer cell conditioned medium (CC-CM) and Co-Culture-CM were collected for ELISA. Each group included triple wells. The experiments were repreated three times (n=9). Human and mouse cytokines and growth factors in these CM were quantified using anti-human or mouse quantitative ELISA kits according to the manufacturer's instructions (R&D, Minneapolis, MN Minneapolis, MN).

Transcription reverse-polymerase chain reaction

Total RNA of cells was extracted using Trizol reagent (Invitrogen, Carlsbad, CA) according to the manufacturer's instructions. RNA concentration was determined by measuring the absorbance at 260 nm (A260) in a spectrophotometer. Complementary deoxyribonucleic acid (cDNA) was synthesized using a reverse transcription kit (Promega). Real-time polymerase chain reaction (real-time PCR) was performed with SYBR green (Thermo Fisher Scientific, Beijing, China) according to the manufacturer's instructions using a Bio-Rad MyiQ Thermal cycler. The sequences of human and mouse primers were as the following: human E-cadherin forward primer 5′-ATCGCTTACACCATCCTCAGCCAA-3′, reverse primer 5′-AGCTGTTGCTGTTGTGCTT AACCC-3′; human snail forward primer 5′-CAATCGGAAGCCTAACTACAGCGA-3′, reverse primer 5′-AG GACAGAGTCCCAGATGAGCATT-3′; human vimentin forward primer 5′-

AGAACCTGCAGGAGGCAGA AGAAT-3′, reverse primer 5′-TTCCATTTCACGCATCTGGCGTTC -3′; human TGF-β1 forward primer 5′-AC ACACTGCAAGTGGACATCAACG-3′, reverse primer 5′-TTCTTCTCCGTGGAGCTGAAG C AA -3′; mouse IL-6 forward primer 5′-CTGCAAGTGCATCATCGTTGTT-3′, reverse primer 5′-CCGGAGAGGAGACTTCA CAGAG-3′; Human CD10 forward Primer 5′-CAACACTCCAAAGCCAAAGAAG-3′, reverse primer 5′-GC TGTCCAAGAAGCACCATA-3′; Human KIAA1199 forward primer 5′-CGGTCTATTCCATCCACATCTC-3′, reverse primer 5′-CCAGACGTTCACTCTCTTTCTT-3′; Human Hey-1, forward primer 5′-AGACCATCG AGGTGGAGAA-3′, reverse primer 5′-TGGGAAGCGTAGTTGTTGAG-3′; Human DUSP6-1 forward primer, 5′-AGCGACTGGAACGAGAATAC-3′, reverse primer 5′-CAAGTAGAGGAAGGGCAAGAT-3′; GAPDH forward primer 5′-GACATCAAGAAGGTGGTGAAGGAG-3′, feverse primer 5′-AACAGGAAATG AGCTTGACAAA -3′. Data were analyzed using the relative standard curve method. Messenger RNA expression levels of the genes were normalized to glyceraldehyde 3-phosphate dehydrogenase (GAPDH). The experiments were repreated three times (n=3).

cDNA Microarray and Bioinformatics Analysis

Total RNA was extracted from MKN28 parental cells and MKN28-CSC-LC spheres. Affymetrix microarray analysis, fragmentation of RNA, labeling, hybridization to Human Genome U133 Plus 2.0 microarrays, and scanning were performed by the Microarray facility of Cancer Institute of New Jersey, Rutgers University, according to the manufacturer's protocol (Affymetrix Santa Clara, CA). Gene expression array data of the NCI-60 cell lines implemented with Affymetix HG-U133A and U133B chip platforms were downloaded from the CellMiner database (http://discover.nci.nih.gov/cellminer/).[5] Heat maps were created using dChip software (http://biosun1.harvard.edu/complab/dchip/). Classical multidimensional scaling was performed using the standard function of the R program to provide a visual impression of how the various sample groups are related. The average-linkage distance was used to assess the similarity of gene expression profiles between MKN28-CLC-LCs and MKN28 parental cells. The error on such a comparison was estimated by combining the standard errors (the standard deviation of pairwise linkages divided by the square root of the number of linkages) of the average-linkage distances involved. Gene annotation was performed by the ArrayFusion web tool (http://microarray.ym.edu.tw/tools/arrayfusion/) and gene enrichment analysis by the DAVID 2008 Bioinformatics Resources (http://david.abcc.ncifcrf.gov/). Array data produced in this work are available from the GEO database (accession no. 16884574).

Flow cytometry

Flow cytometry was performed on trypsin-dissociated spheres. Cells suspensions were stained with fluorescence-labeled anti-CD44 (BD Biosciences, Cat. 553133, 1:100), then subjected to flow cytometry (FACS) analysis using FACS 500 or MoFlo cell sorter (Beckman Coulter) at the Cytometry and Imaging Core Facility. Dead cells were excluded with propidium iodide staining. All antibodies for FACS analysis were purchased from e-Biosciences. Data were analyzed using the Summit software (Beckman Coulter). The experiments were repreated three times (n=3).

Western blot

Cancer cells and BMFs were lysed with lysis buffer. Protein samples were subjected to SDS-polyacrylamide gels (Bio-Rad) electrophoresis. The gels were transferred onto nitrocellulose membranes (Bio-Rad). The membranes were probed with specific primary antibodies against JAK2 (Cat. 3230S), p-JAK2 (Cat. 3771S), STAT3 (Cat. 9139S), p-STAT3-Y705 (Cat. 76315), Met (Cat. 8198), p-Met (Cat. 3077), Smad2/3 (Cat. 5678), p-Smad2 (Cat. 8828), vimentin (Cat. 3879) (Cell signaling Technology), snail (Cat. 92547), E-cadherin (Cat. ab15148), TGF-β1 (Cat. ab66043), and IL-6 (Cat. ab6672), and β-actin (Cat. ab6276) (Abcam), incubated with secondary antibodies conjugated to IR fluorophore, Alexa Fluor 680 (Molecular Probes), or IRdye 800 (Rockland Immunochemicals). Antigen-antibody complexes were visualized by the ECL system (Amersham Biosciences, Piscataway, NJ) and scanned using the Odyssey Infrared Imaging System (Li-Cor Biosciences). The experiments were repreated three times (n=3).

Immunohistochemistry and tissue array

Tissue array samples of human gastric cancer were from Shanghai Ruijin Hospital, Shanghai Jiaotong University School of Medicine. The tissue array section included 41 gastric cancer tissues and 10 normal gastric tissues. The study was performed according to the guidelines of the Medical Ethics Committee of Shanghai Jiaotong University School of Medicine in China and written informed consent was obtained from all patients at study entry. Tissues were formalin-fixed, dehydrated and embedded in paraffin. Immunohistochemical staining was performed as described previously [30]. In brief, the tissues sections were deparaffinized, rehydrated and boiled in 0.01M sodium citrate, pH 6.0 for antigen retrieval. The endogenous peroxidase activity was quenched. The sections were incubated with anti-TGF-β1 antibody (Abcam, Cat. ab66043), anti-IL-6 antibody (Abcam ab6672) or anti-HGF antibody (Abcam, Cat. ab189511) overnight at 4°C. Tumor sections were incubated with biotinylated secondary antibodies, streptavidin-biotin complex (Dako, Glostrup, Denmark). Staining was visualized using diaminobenzidine. Representative photos were taken with a Nikon Eclipse E800 microscope equipped with a Nikon DXM1200 digital camera (Nikon instruments, Melville, NY, USA). The result of the immunohistochemistry for gene expression was judged based on the extent and intensity of staining as follows: (1) The extent of positive cells was estimated as 0   5%, 1 = 6-25%, 2 = 26-50%, 3 = 51-75%, 4   75%. (2) The intensity of staining was judged as 0 = achromatic, 1 = light yellow, 2 = yellow, 3 = brown. The score of the extent of positive cells was multiplied by the score of the intensity of staining, and the combined staining score as follows : (−) = 0, (+) = 1-4, (++) = 5-8, (+++) = 9-12. Specimens were considered to have low expression of proteins when the score was 0 or +, and were considered to have high expression for genes when the score was ++ or +++. This semi-quantitative analysis was done by two independent assessors without prior to knowledge of the patient outcome.

Immunofluorescence staining

Frozen xenograft tumor sections (5 um) were subjected to double-immunofluorescence staining by simultaneous incubation of sections with mouse anti-EGFP antibody (Abcam Cat. Ab184601) and rabbit anti-αSMA antibody (Abcam, Cat. 5694) overnight at 4°C and

then incubated with FITC-conjugated anti-mouse secondary antibody and Cy3 red-conjugated anti-rabbit secondary antibody (Vector Laboratories) for 1 hour at room temperature. Slides were counterstained with 2 mg/ml DAPI (Vector Laboratories). Specimens were observed with an Olympus FluoView confocal microscope, and images were analyzed with Adobe Photoshop. The numbers of DAPI$^+$ cells, EGFP$^+$ cells and /or α-SMA$^+$ were counted under × 400 magnification in five random chosen fields. BMFs fluoresced yellow because of the overlapping green and red emissions. Percentage of positive cells was expressed as an average of the ratios of positive staining cells to the total DAPI positive number in 5 random at 400 magnification from tumor sections of three mice (n=15).

Tumor xenograft models

Five-week old femal healthy athymic nude or NOD/SCID mice from Harlan Laboratories (Indianapolis, IN) were maintained in a sterilized animal room at our animal facility. Mice were randomly divided into different groups and were then injected with different cells. Cancer cells were injected subcutaneously (*s.c.*) alone or together with BMFs into both flanks of the mice following the Protocol No. 09-050 supervised by the Institutional Animal Care and Use Committee of the Ethics Committee. Each group included 5 mice with 10 injection sites (n=10). For the injection of spheroid cells, the spheres were digested to single cells and suspended in PBS. Spheroid cells were injected *s.c.* both flanks of into NOD/SCID mice. Each group included 5 mice with 10 site injections (n=10). For the injections of MKN28-STAT3-shRNA cells, each group included 4 mice with 8 site injections (n=8). For the injections of different number of MKN28-parentalcells, each group included 3 mice with 6 site injections (n=6). Tumor size was measured weekly by two researchers without knowledge of cells injected. tumor development was monitored for 3 months. When the tumor size reached 2 cm^3, mice were killed, and tumors were processed for histological and immunohistochemical analyses.

Statistical analysis

Unless indicated otherwise, all experiments were repeated three times. Power calculations were performed for animal studies, and the number of mice reflects the number needed to have sufficient power (80%) to measure the expected difference (20%) in the incidences of tumor formation at p < 0.05. Based on our preliminary studies, the numbers of animals are included. Results were expressed as Means ± SD. Differences between 2 groups was analyzed for using a 2-tailed Student *t* test for assuming equal variances, with a *P* value less than 0.05 deemed significant. The χ^2 test was applied for comparison of dichotomous variables. One-way ANOVA test was used for comparing the results of 3 or more groups. All statistical analyses were performed using SPSS 22.0 software (SPSS Inc, Chicago, IL, USA).

Supplementary Material

Refer to Web version on PubMed Central for supplementary material.

Author Manuscript

Author Manuscript

Author Manuscript

Author Manuscript

Acknowledgements

Abbreviations

BMFs	bone marrow-derived myofibroblasts
BMF-CM	BMF conditioned medium
Co-culture-CM	co-culture medium of BMFs and cancer cells
IL-6	interleukin-6
JAK2	janus kinase2
STAT3	signal transducer and activator of transcription 3
HGF	hepatocyte growth factor
CAFs	cancer-associated fibroblasts
MSCs	mesenchymal stem cells
EGF	epithelial growth factor
bFGF	basic fibroblast growth factor
TGF-β	transformation growth factor-β
CSCs	cancer stem cells
CSC-LCs	CSC-like cells
FACS	flow cytometry
ELISA	enzyme-linked immunosorbent assays

References

1. Double blind controlled phase III multicenter clinical trial with interferon gamma in rheumatoid arthritis. German Lymphokine Study Group. Rheumatol Int. 1992; 12:175–185. [PubMed: 1290019]

2. Beppu H, Mwizerwa ON, Beppu Y, Dattwyler MP, Lauwers GY, Bloch KD, et al. Stromal inactivation of BMPRII leads to colorectal epithelial overgrowth and polyp formation. Oncogene. 2008; 27:1063–1070. [PubMed: 17700526]

3. Bhowmick NA, Neilson EG, Moses HL. Stromal fibroblasts in cancer initiation and progression. Nature. 2004; 432:332–337. [PubMed: 15549095]

4. Birkenkamp-Demtroder K, Maghnouj A, Mansilla F, Thorsen K, Andersen C, Ãšter B, et al. Repression of KIAA1199 attenuates Wnt-signalling and decreases the proliferation of colon cancer cells. British journal of cancer. 105:552–561.

5. Calon A, Espinet E, Palomo-Ponce S, Tauriello DV, Iglesias M, Cespedes MV, et al. Dependency of colorectal cancer on a TGF-beta-driven program in stromal cells for metastasis initiation. Cancer Cell. 2012; 22:571–584. [PubMed: 23153532]

6. Castano Z, Fillmore CM, Kim CF, McAllister SS. The bed and the bugs: interactions between the tumor microenvironment and cancer stem cells. Semin Cancer Biol. 22:462–470.

7. Erez N, Truitt M, Olson P, Arron ST, Hanahan D. Cancer-Associated Fibroblasts Are Activated in Incipient Neoplasia to Orchestrate Tumor-Promoting Inflammation in an NF-kappaB-Dependent Manner. Cancer Cell. 17:135–147.

8. Giraud AS, Menheniott TR, Judd LM. Targeting STAT3 in gastric cancer. Expert Opinion on Therapeutic Targets. 16:889–901.

9. Gomes I, Mathur SK, Espenshade BM, Mori Y, Varga J, Ackerman SJ. Eosinophil-fibroblast interactions induce fibroblast IL-6 secretion and extracellular matrix gene expression: implications in fibrogenesis. Journal of allergy and clinical immunology. 2005; 116:796–804. [PubMed: 16210053]

10. Hamerlik P, Lathia JD, Rasmussen R, Wu Q, Bartkova J, Lee M, et al. Autocrine VEGF-VEGFR2-Neuropilin-1 signaling promotes glioma stem-like cell viability and tumor growth. J Exp Med. 209:507–520.

11. Hammacher A, Ward LD, Simpson RJ, Weinstock J, Treutlein H, Yasukawa K. Structure-Function analysis of human IL-6: Identification of two distinct regions that are important for receptor binding. Protein Science. 1994; 3:2280–2293. [PubMed: 7538847]

12. Hawinkels LJ, Paauwe M, Verspaget HW, Wiercinska E, van der Zon JM, van der Ploeg K, et al. Interaction with colon cancer cells hyperactivates TGF-beta signaling in cancer-associated fibroblasts. Oncogene. 2012

13. Hayward SW, Wang Y, Cao M, Hom YK, Zhang B, Grossfeld GD, et al. Malignant transformation in a nontumorigenic human prostatic epithelial cell line. Cancer Res. 2001; 61:8135–8142. [PubMed: 11719442]

14. Jinushi M, Chiba S, Yoshiyama H, Masutomi K, Kinoshita I, Dosaka-Akita H, et al. Tumor-associated macrophages regulate tumorigenicity and anticancer drug responses of cancer stem/initiating cells. Proc Natl Acad Sci U S A. 108:12425–12430.

15. Kalluri R, Zeisberg M. Fibroblasts in cancer. Nature Reviews Cancer. 2006; 6:392–401. [PubMed: 16572188]

16. Kaplan RN, Rafii S, Lyden D. Preparing the "soil": the premetastatic niche. Cancer Res. 2006; 66:11089–11093. [PubMed: 17145848]

17. Lecomte J, Masset A, Blacher S, Maertens L, Gothot A, Delgaudine M, et al. Bone marrow-derived myofibroblasts are the providers of pro-invasive matrix metalloproteinase 13 in primary tumor. Neoplasia. 2012; 14:943–951. [PubMed: 23097628]

18. Lee BS, Park M, Cha HY, Lee JH. Hepatocyte growth factor induces delayed STAT3 phosphorylation through interleukin-6 expression. Cell Signal. 2009; 21:419–427. [PubMed: 19071214]

19. Liu X, Yao W, Newton RC, Scherle PA. Targeting the c-MET signaling pathway for cancer therapy. Expert Opin Investig Drugs. 2008; 17:997–1011.

20. Maguerâ€Satta V, BesanÃ§on R, Bachelardâ€Cascales E. Concise review: neutral endopeptidase (CD10): a multifaceted environment actor in stem cells, physiological mechanisms, and cancer. Stem Cells. 29:389–396.

21. Malanchi I, Santamaria-Martinez A, Susanto E, Peng H, Lehr HA, Delaloye JF, et al. Interactions between cancer stem cells and their niche govern metastatic colonization. Nature. 481:85–89.

22. Mani SA, Guo W, Liao MJ, Eaton EN, Ayyanan A, Zhou AY, et al. The epithelial-mesenchymal transition generates cells with properties of stem cells. Cell. 2008; 133:704–715. [PubMed: 18485877]

23. Nguyen LV, Vanner R, Dirks P, Eaves CJ. Cancer stem cells: an evolving concept. Nat Rev Cancer. 12:133–143.

24. Powell DW, Adegboyega PA, Di Mari JF, Mifflin RC. Epithelial cells and their neighbors I. Role of intestinal myofibroblasts in development, repair, and cancer. Am J Physiol Gastrointest Liver Physiol. 2005; 289:G2–7. [PubMed: 15961883]

25. Quante M, Tu SP, Tomita H, Gonda T, Wang SS, Takashi S, et al. Bone marrow-derived myofibroblasts contribute to the mesenchymal stem cell niche and promote tumor growth. Cancer Cell. 2011; 19:257–272. [PubMed: 21316604]

26. Scheel C, Weinberg RA. Cancer stem cells and epithelial-mesenchymal transition: concepts and molecular links. Semin Cancer Biol. 22:396–403.

27. Takishi S, Okumura T, Tu SP, Wang SW, Shibata W, Vigneshwaran S, et al. Identification of gastric cancer stem cells using the cell surfae marker CD44. Stem Cells. 2009; 27:1006–20. [PubMed: 19415765]

28. Tsai KS, Yang SH, Lei YP, Tsai CC, Chen HW, Hsu CY, et al. Mesenchymal stem cells promote formation of colorectal tumors in mice. Gastroenterology. 141:1046–1056.

29. Tu S, Bhagat G, Cui G, Takaishi S, Kurt-Jones EA, Rickman B, et al. Overexpression of interleukin-1beta induces gastric inflammation and cancer and mobilizes myeloid-derived suppressor cells in mice. Cancer Cell. 2008; 14:408–419. [PubMed: 18977329]

30. Tu SP, Jiang XH, Lin MC, Cui JT, Yang Y, Lum CT, et al. Suppression of survivin expression inhibits in vivo tumorigenicity and angiogenesis in gastric cancer. Cancer research. 2003; 63:7724–7732. [PubMed: 14633697]

31. Vermeulen L, De Sousa EMF, van der Heijden M, Cameron K, de Jong JH, Borovski T, et al. Wnt activity defines colon cancer stem cells and is regulated by the microenvironment. Nat Cell Biol. 12:468–476.

32. Visvader JE, Lindeman GJ. Cancer stem cells in solid tumours: accumulating evidence and unresolved questions. Nat Rev Cancer. 2008; 8:755–768. [PubMed: 18784658]

33. Watabe T, Miyazono K. Roles of TGF-Î2 family signaling in stem cell renewal and differentiation. Cell research. 2008; 19:103–115.

34. Xu J, Lamouille S, Derynck R. TGF-Î2-induced epithelial to mesenchymal transition. Cell research. 2009; 19:156–172. [PubMed: 19153598]
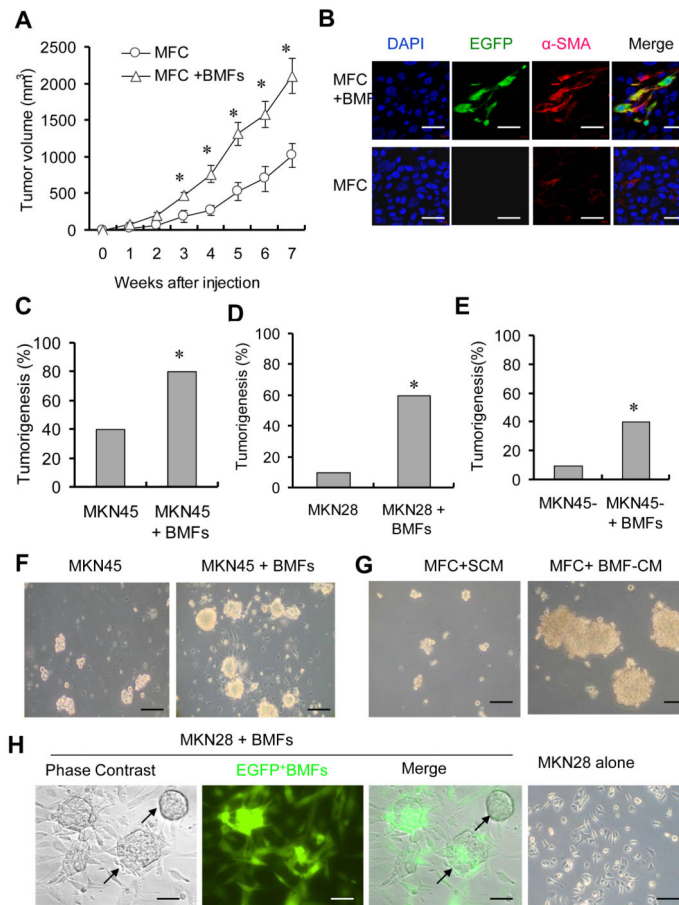
Fig. 1. BMFs enhance tumorigenesis in gastric cancer cells

(**A**) Mouse gastric cancer MFC cells (1×10^4) were injected *s.c.* alone or together with BMFs (1×10^4) into the both flanks of nude mice. Each group include 5 mice (10 injection sites, n=10). Tumor size was measured weekly. Tumor growth curve was shown accordingly . *P<0.01, compared to MFC cells alone group. (**B**) The expression of EGFP and α-SMA was determined by immuofluorescence staining in xenograft tumor tissues from mice injected with MFC cells alone or together with BMFs (scale bar, 50 μM). (**C-E**) Highly tumorigenic gastric cancer MKN45 cells, weakly tumorigenic MKN28 cells and sorted CD44⁻ MKN45 cells (10^4 cells) were injected (*s.c.*) alone or co-injected with BMFs (10^4) into both flank of mice (each group included 5 mice with 10 injection sites) in each experiment. Tumor growth was monitored each week for 3 months. The rate of tumor formation presented was from 5 mice with 10 injection sites each group (n=10). *P<0.01, compared to MKN45 cells alone group. (**F**) MKN45 cells were cultured alone or co-cultured with BMFs in SCM in attachment 6-well plates for 2 weeks. (**G**) Mouse gastric cancer cells MFC were cultured in SCM, BMF-CnM or Co-culture-CM in an ultralow attachment 96-well plate for 2 weeks. Representative sphere photos were taken on day 14 (*scale bar*, 100 μM). (**H**) MKN28 (EGFP⁻) cells were cultured alone or with BMFs (EGFP⁺) for 2 weeks. All representative sphere photos were taken on day 14 (*scale bar*, 100 μM).
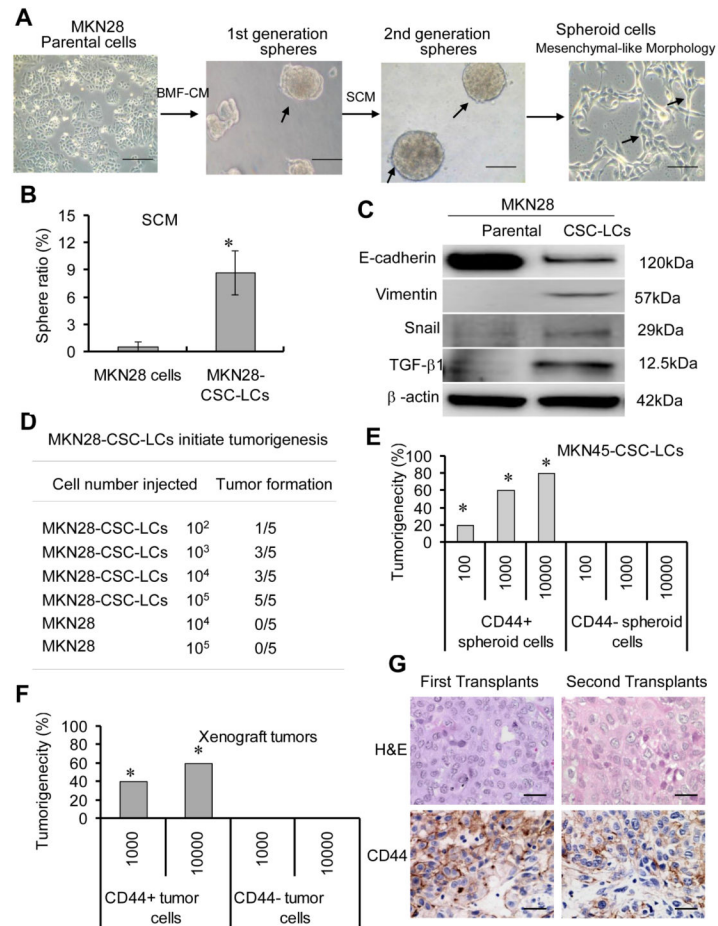
Fig. 2.
BMF-induced spheres exhibit CSC properties. (**A**) Single spheroid cells isolated from BMF-CM-induced first generation spheres (*second panel*) were cultured in an ultralow attachment 96-well plate for 2 weeks and formed second generation spheres (*third panel*). The second generation spheroid cells were cultured in attachment plates and exhibited fibroblast-like morphology *(fourth panel)* (*scale bar*, 50 μM). (**B**) MKN28 cells and single MKN28-CLC-LCs were cultured in a 96-well plate in SCM for 2 weeks. Sphere ratio is means ± SD of 3 independent experiments. *$P < 0.01$, compared to MKN28 parental cells. (**C**) Protein expressions of EMT-related genes in indicated cells were determined by Western Blot. (**D**) MKN28-CSC-LCs and MKN28-parental cells at indicated cell numbers were injected into the flanks of athymic nude mice (n=5). Tumor formation was monitored for 3 months. (**E**) Sorted CD44$^+$ and CD44$^-$ MKN45 cells from MKN45-CSC-LCs at indicated numbers were injected *s.c.* into the both flanks of nude mice (n=5). Tumor formation was monitored for 3 months. The percentage of mice with tumors was shown. *$P < 0.01$, compared to CD44$^-$ cells. (**F**) Sorted CD44$^+$ and CD44$^-$ tumor cells from xenograft tumors at indicated numbers were injected *s.c.* into the flanks of nude mice (n=5). Tumor formation was monitored for 3 months. The percentage of mice with tumors is shown.*$P < 0.01$, compared to CD44$^-$ cells. (**G**) First and second transplants tumor tissues were suffered H&E and CD44 staining.
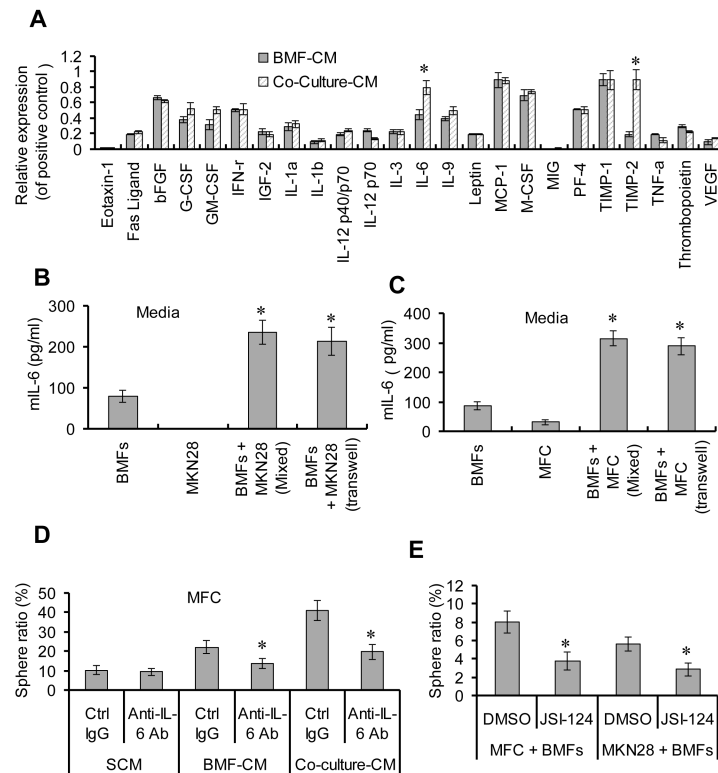
Fig. 3.

BMF-derived IL-6 induces sphere formation of mouse cancer cells. (**A**) BMFs were cultured alone or co-cultured with MKN28 cells in serum-free media for 48 hours. The levels of various factors in culture media were measured by antibody array assay and were normalized to positive control, which is the reagents in the kit which is from Ray Biotech Company. Data are expressed as fold inductions from duplicate experiments. (**B-C**) BMFs were cultured alone, mixed co-cultured, or co-cultured in a transwell system with MKN28 cells (**B**) and MFC cells (**C**) for 48 hours. The mIL-6 level in the media was measured by anti-mouse IL-6 ELISA kit. (**D**) Mouse MFC cells were cultured for 2 weeks with SCM, BMF-CM or Co-Culture-CM that has been pre-incubated with anti-mouse IL-6 neutralizing antibody or control IgG. (**E**) MFC cells and MKN28 cells were co-cultured with BMFs in the presence or absence of JSI-124 (0.25 μM) for 2 weeks. All sphere ratios are means ± SD of 3 independent experiments. *$P < 0.05$, compared to the control groups.
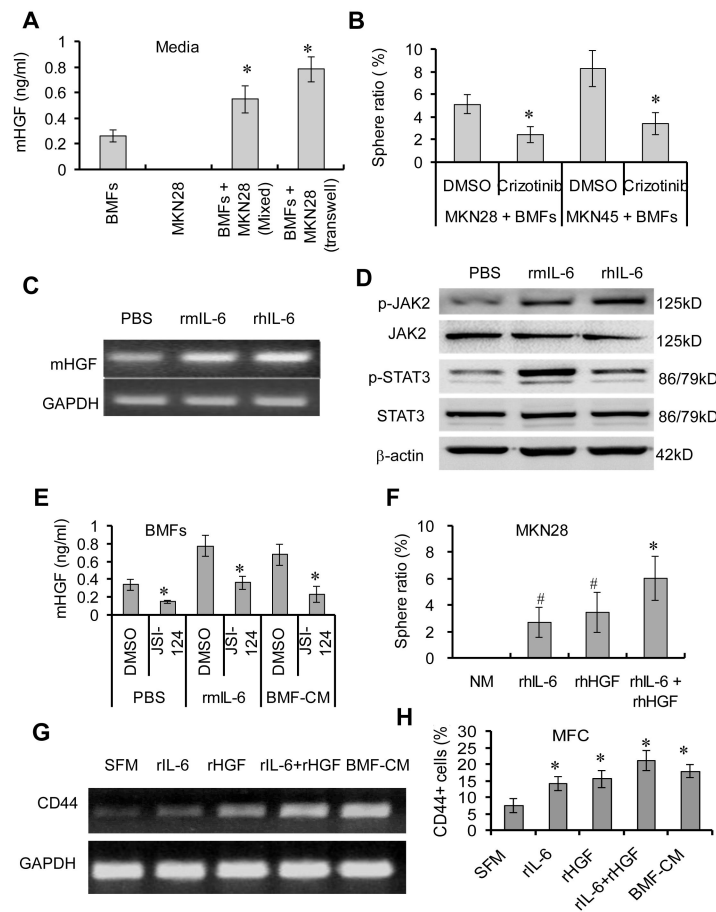
Fig. 4.
BMF-derived HGF contributes to the sphere formation of human cancer cells. (**A**) BMFs were mixed co-cultured or in a transwell system with MKN28 cells in 2 ml of media for 48 hours. The mHGF level in the media was determined by ELISA. (**B**) MKN28 and MKN45 cells were co-cultured with BMFs in SCM in the presence or absence of crizotinib (1.00 μM) for 2 weeks. $*P<0.05$, compared to DMSO group. (**C**) BMFs were treated with rIL-6 for 48 hours and the HGF mRNA expression was determined by RT-PCR. (**D**) BMFs were treated with rIL-6 for 10 min. The protein expression was determined by Western Blot. (**E**) BMFs were treated with rhIL-6 or BMF-CM in the presence or absence of JSI-124 (0.25 μM) for 48 hours. mIL-6 level was measured by ELISA. $*P< 0.01$, compared to the vehicle control. MKN28 cells were treated with rhIL-6 (20 ng/mL), rhHGF (20 ng/mL) or their combination (20 ng/mL, each) in normal media(NM) for 2 weeks. Sphere ratio is means ± SD from 3 independent experiments. $*P< 0.05$, compared to rhIL-6 and rhHGF treatment alone; $\#P<0.05$, compared to NM group. (**G-H**) MFC cells were treated with indicated factors or medium for 24 hours. mRNA expression of CD44 was determined by RT-PCR (**H**) and percentages of CD44+ was determined by FACS. $*P< 0.05$, compared to Serum-Free Media (SFM) treatment.
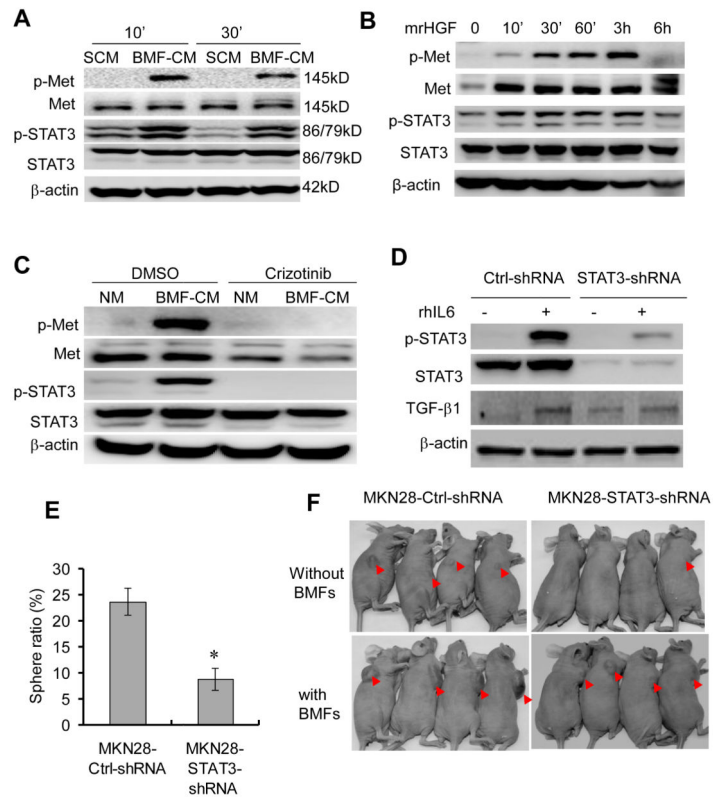
Fig. 5.
The activation of STAT3 and Met contributes to BMF-induced sphere formation and tumorigenesis. Human gastric cancer MKN28 cells were cultured in SCM or BMF-CM (**A**) or rmHGF (20 ng/mL) (**B**) in indicated time. (**C**) Cancer cells were treated with BMF-CM in presence or absence of crizotinib (20 μM) for 2 hours. All protein expression was determined by Western Blot. (**D**) Stable MKN28-STAT3-shRNA and MKN28-Ctrl-shRNA cells were treated with rhIL-6 (20 ng/mL) for 48 hours. Protein expression was detected by Western Blot. (**E**) Stable MKN28-STAT3-shRNA and MKN28-Ctrl-ShRNA cells were cultured in BMFCM in 96-well plates for 2 weeks. The sphere ratio is the means ± SD of 3 independent experiments. (**F**) The MKN28-STAT3-shRNA and MKN28-Ctrl-ShRNA cells were injected *s.c.* alone or together with BMFs into the both flanks of nude mice (n=4 mice, 8 injection sites). The representative photos were taken in week 5 from one of two experiments.
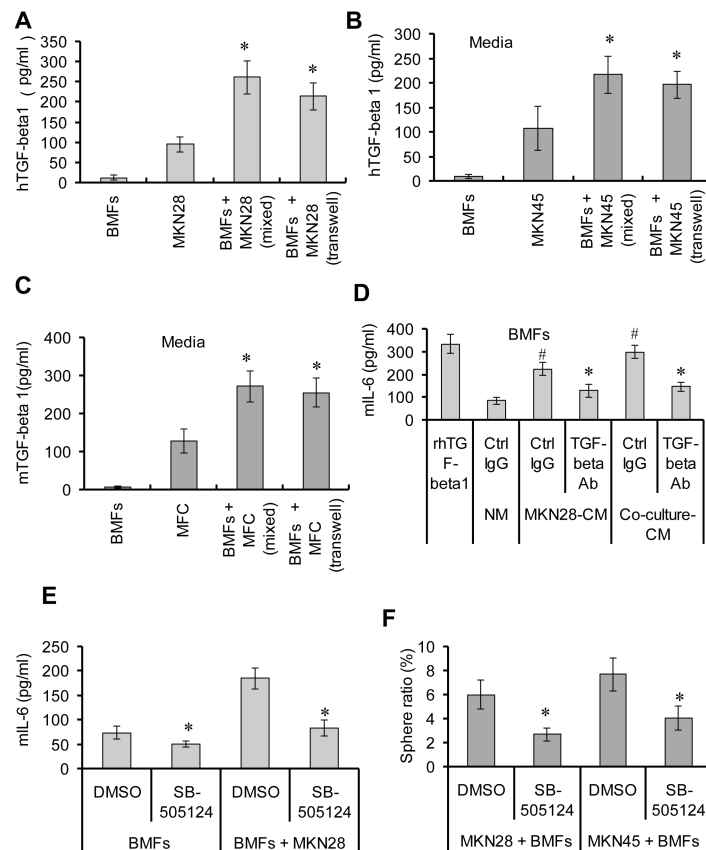
Fig. 6.
MKN28 cells (**A**), MKN45 (**B**) or MFC (**C**) were cultured alone or co-cultured mixedly or in a transwell system with BMFs cells for 48 hours. The hTGF-β1 level in the media was measured by anti-human TGF-β1 ELISA kit. *P< 0.01, compared to cancer cell culture alones. Cancer cell-derived TGF-β1 activates BMFs. (**D**) The BMFs were treated with rhTGF-β1, MKN28-CM or Co-culture-CM in the presence or absence of anti-human TGF-β1 neutralizing antibody for 48 hours. *P< 0.01, compared to control IgG. #P< .01, compared to NM. (**E**) BMFs were cultured alone or with MKN28 cells in the presence or absence of SB-505124 for 48 hours. The mIL-6 level was measured by ELISA. *P< 0.01, compared to control groups. (F) MKN28 or MKN45 were co-cultured with BMFs with and without SB-505124 in SCM for 2 weeks. Sphere ratio is the means ± SD of 3 independent experiments. *P< 0.01, compared to control groups.
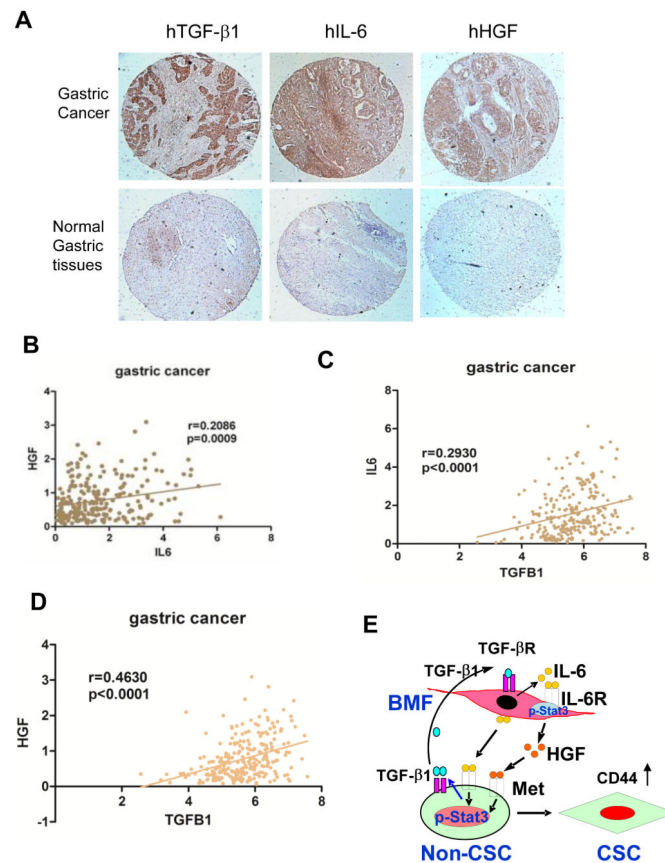
Fig. 7.
The correlations among expressions of hTGF-β1, hIL-6 and hHGF in human gastric cancer tissues. (**A**) Expressions of hTGF-β1, HGF and hIL-6 in human gastric cancer tissues array samples were determined by IHC with anti-human TGF-β1, HGF and IL-6 antibodies using. (**B-D**) Association analysis of mRNA expression of hTGF-β1, hHGF and hIL-6 in NIH TCGA gastric cancer database. (**E**) A model for the interactions between BMFs and cancer cells through an IL-6/HGF and TGF-β1 signaling loop.